Dynamic Analysis of Cancer-Immune System with Allee Effect

by

© **Cuiping Wang**

A thesis submitted to the School of Graduate Studies in partial fulfillment of the requirements for the degree of Master of Science.

Department of Mathematics and Statistics

Memorial University

October 2021

St. John's, Newfoundland and Labrador, Canada

Abstract

There are numbers of mathematical models to describe the relation between immune effector cells and cancer cells. The purpose of this thesis is to explore the influence of Allee effect on immune effector cells and cancer cells.

First, we introduce some background information of how the immune system inhibit and suppress cancer growth and Allee effect.

In Chapter 2, we propose a general model to describe the interaction between immune effector cells and cancers. We discuss some basic dynamical properties of the system under strong Allee effect and weak Allee effect with linear functional responses. For instance, the existence of equilibrium points and their local stabilities.

In Chapter 3, using Matlab code, we do sampling-based sensitive analysis on the density of cancer cells. Sensitive analysis can narrow down the parameter of interest and suggest the most significant parameter that affect the density of cancer cells.

In Chapter 4, due to the difficulty of solving the explicit form of positive equilibrium point. We give numerical simulation to explore the existence of positive equilibrium points and their stabilities.

At last, in Chapter 5, we summarize the results in this thesis, and indicate some problems for future work.

To whom you what to dedicate this work

Lay summary

Cancer has become a leading cause of death worldwide and has deeply impact on millions of people's life. In order to provide therapies for patients, it is very important for researchers to understand how the immune system fight against with cancer cells. In this thesis, we build a mathematic model to study the interaction between immune effector cells and cancer cells. We introduce Allee effect on immune effector cells and cancer cells to see its influence. We perform sensitivity analysis to find the most influential parameters in the model.

Acknowledgements

I would like to thank my supervisor Prof. Yuan for her devotion, guidance and support throughout the course of my program. She patiently reads my work and answer to all my questions.

I would like to thank Prof. Xiaoqiang Zhao, Prof. Jie Xiao and Prof.Chunhua Ou for teaching me dynamical systems and analysis.

Thanks to my professor Yuan Yuan for the financial support and the Department of Mathematics and Statistics for providing me teaching assistant fellowship.

I would like to thank all staff members at the Department of Mathematics and Statistics. They are very nice and helpful.

I am very appreciate my friend Daifeng Duan who encourage me to do difficult projects and provide valuable help with my study.

Statement of contributions

Under the supervision of Dr. Yuan, I have derived the conditions for the existence of the equlibium points and their local stalibity. In addition I have done the sensitity analysis with parameters and numerical simulations.

Table of contents

List of tables

List of figures

List of symbols

$N(\mu, \sigma^2)$	normal distribution with mean μ and variance σ^2
R	real numbers

List of abbreviations

WHO	World Health Organizaton
LHS	Latin Hypercube sampling
CC	Pearson correlation coefficient
PCC	Partial correlation coefficient
PRCC	Partial rank correlation coefficients.

Chapter 1

Introduction and Preliminaries

1.1 Introduction

It is known that cancer is an evolutionary process and has been widely thought to originate from mutation and an inhibition of growth suppressors. What is worse is the cell proliferation and the risk of metastasis. It has become a leading cause of death worldwide. Millions of people's life has been deeply affected by cancer every year and its impact continues to increase. According the report by World Health Organizaton in 2021 (WHO), there were approximately 10.1 million people living with cancer around the world in 2020 and 5.019 million people died from cancer throughout the world in 2020 [29].

Immune system plays a vital role in inhibiting or suppressing tumor growth. One of the major challenges of the twenty-first century for scientists in immunology and cancer research is to fully understand how the immune system affects cancer development and progression [27]. In 1909, Paul Ehrlich [31] first suggested that cancer can occur in vivo suddenly and our body could generate immunity against cancer. The immune response for the cancer indicates that there exists unique molecules that can recognize and protect against specific cancer. In the late 1950s, based on the studies of the cellular basis of transplantation and tumor immunity, Burnet [1] and Thomas [2] proposed that complex organisms possessed a system that can recognizes and destroys continuously arising nascent transformed cells and postulated the concept of *cancer immunosurveillance*. Data obtained from the studies on both mice

and humans with cancer suggest that there were several factors can suppress tumor growth by destroying cancer cells or inhibiting their outgrowth such as innate and adaptive immune cell types, effector molecules, and pathways. On the other hand, the immune system can also promote tumor progression from two sides: one by selecting for tumor cells that are more fit to survive in an immunocompetent host; another by establishing conditions within the tumor microenvironment that facilitate tumor outgrowth (Dunn et al. [3], Matsushita et al. [7], Mohme et al. [11], Pardoll et al. [12], Schreiber et al. [27], Vesely et al. [18]). Immune system can both suppress and promote tumor growth. This dual role of immune system is termed *cancer immunoediting*, which consists of three processes: elimination (immunity functions as an extrinsic tumor suppressor in naive hosts); equilibrium (expansion of transformed cells is held in check by immunity); and escape (tumor cells attenuate immune responses and grow into cancers)(Dunn et al. [3, 5], Koebel et al. [17], Schreiber et al. [27]).

One of the most vital components of the immune system in the process of fighting against cancer is T cells . Generally, T cells originate from hematopoietic stem cells in the bone marrow. CD8+ T cells, also known as "killer T cells" , are cytotoxic T cells. These T cells can directly kill virus-infected cells, as well as cancer cells and also can produce cytokines IL-2 and $IFN\gamma$ which can influence the effector functions of other cells, in particular macrophages and NK cells. In order to have the ability of killing cancer cells, the naive T cells move to the lymph nodes where they can be activated after contacting with cognate antigens. Activated T cells will proliferate rapidly and be transported to the tumour site through the blood vessels to kill the infected cells.

It is known that Allee effect is a biological phenomenon characterized by positive association between population size or density and absolute average individual fitness. There are two types of Allee effect: strong or weak. When Allee effects are strong, populations less than threshold will decline to extinction. When Allee effects are weak, the growth rate of population always remains positive.

Cancers growth has been assumed as cell autonomous proliferation, manifested as exponential increase in cell number, and limited by the carrying capacity. However, an increasing number of studies show that, in some cases, cell population kinetics are best described by considering processes models involving the Allee effect, we refer: Johnson [32], Korolev [33], Neufeld [28] for more details. A variety of mechanisms may be the reason that cause Allee effect such as cooperative interactions (Korolev

[33]). Cooperation is common to a wide variety of organisms. In cancer, cooperation might be needed to produce sufficient growth factors which guarante the proliferation of tumor (Korolev [33]). Some mathematical models with Allee effect have been presented in Böttger [34], Konstorum [26] and the impact of Allee effect in spreading of cancer cells has been investigated in Feng [19], Sewalt [6]. Studies show that there is Allee effect phenomenon on the dynamics of immune effectors. That is because immune system can weaken at some times, either by the presence of other disease, or due to a bad nutrition (Mckenzie [8], Kirchner [9]). Thus, there is a threshold. If the immune effector density is greater than this threshold, it will converge to carrying capacity. This assumption on the dynamics of immune effectors may be useful to evaluate the impact of the immune effectors on the disease progression.

Mathematical models provide a useful method and framework to investigate and solve real world problems. In the context of dynamics system, through the mathematical analysis, we maybe able to predict the development direction in advance and propose an effective measure to prevent the spread of tumor and control tumor growth. There exist several handful of compartmental mathematical models of cancer dynamics (Kirschner and Panetta [14], Kuznetsov et al. [42], Owen and Sherratt [21]) to study the interaction between tumor and immune system. However, few achievements consider Allee effects both on immune effector cells and tumor cells.

Sensitivity analysis (SA) is a method to quantify uncertainty and examine how the critical parameters affect outcomes. The Pearson correlation coefficient (CC) provides a measure of the strength of a linear relationship between input parameters and an outcome in a model. The problem is that CC is limited to quantify the association between two variables. It does not account the impact of the other parameters on output variable by showing the degree of monotonicity between specific input parameters and corresponding output variable.

Partial correlation coefficient (PCC) is a more appropriate measure to explore the sensitivity. In fact, after discounting the linear effects of the Latin Hypercube Sampling (LHS) parameters on the outcome, Partial Correlation Coefficient quantify the linear relationship between the LHS parameters and the outcome (Marino [39]). It does not widely apply to the type of sensitivity analysis when the outcome measures has a nonlinear relationship with input parameters or variables.

Partial rank correlation coefficients (PRCC) provides a robust sensitivity measure

for nonlinear, but monotonic, relationships between the output and each of the independent parameters (Marino [39]), Saltelli [47]). PRCC is also a powerful techniques to analyze the sensitivity of a parameter that is strongly monotonic yet highly nonlinear, regardless of whether the parameter has a positive or negative influence on the outcome variable.

1.2 Preliminaries

In mathematics, a function which describes the time dependence of a point in a geometrical space is called a dynamical system.

Differential equations is the most widely used methods to describe and investigate a system that changes over time. It provides a better approach to analyze the long time behavior of dynamical system, to discover the factor that cause the change of behavior and improve the good behavior of the system. The origination of the behavior of a system generally is the structure of dynamic system. Feedback loops, accumulations and flows, nonlinear behavior created by the interaction of structure consist the structure of a system (Sterman [23]).

In this thesis, we mainly discuss the equilibrium points, stability of dynamical systems. Zero change is one of the most important forms of change, i.e. stability, where the dynamics could recreate its preceding state into the current state.

An equilibrium solution of a general autonomous system

$$\dot{x} = f(x), \quad x \in \mathbb{R}^n. \tag{1.1}$$

is a point $\bar{x} \in \mathbb{R}^n$ such that $f(\bar{x}) = 0$.

To determine the stability of equilibrium points we generally linearize the system (1.1) at the equilibrium points $\bar{x}$ and obtain the linear system

$$\dot{y} = Df(\bar{x})y,$$

where $Df = [\partial f_i/\partial x_j]$ is the Jacobian matrix of first partial derivatives of the function $f = (f_1(x_1, \ldots, x_n), f_2(x_1, \ldots, x_n), \ldots, f_n(x_1, \ldots, x_n))^T$ (T denotes transpose).

The local stability analysis of hyperbolic equilibrium points can be done based

upon the standard linearization technique and using the Jacobian matrix.

The characteristic equation is

$$|\lambda - Df(\bar{x})| = 0$$

Then, we have the following theorem:

Theorem 1. *Suppose all of the eigenvalues $\lambda_1, \ldots, \lambda_n$ of $Df(\bar{x})$ have negative real parts. Then the equilibrium solution $x = \bar{x}$ of the vector field (1.1) is asymptotically stable [22].*

Consider a characteristic polynomial with real coefficients:

$$p(\lambda) = a_0\lambda^n + a_1\lambda^{n-1} + \cdots + a_{n-1}\lambda + a_n, \quad a_i \in \mathbb{R}, a_0 \neq 0. \tag{1.2}$$

Generally, we can not obtain an explicit form of λ by solving characteristic equation. We introduce the following theorem which study the roots of characteristic polynomials by exploring the coefficients.

Theorem 2. *(***Descartes' Rule of Sign***) Consider the sequence of coefficients of (1.2):*

$$a_n, a_{n-1}, \cdots, a_1, a_0.$$

Let k be the total number of sign changes from one coefficient to the next in the sequence. Then the number of positive real roots of the polynomial is either equal to k, or k minus a positive even integer [22],. (Note: if $k = 1$ then there is exactly one positive real root.)

First we construct the Routh table associated with the polynomial (1.2) [22]. This is given by:

$$\begin{array}{ccccc}
a_0 & a_2 & a_4 & a_6 & \cdots \\
a_1 & a_3 & a_5 & a_7 & \cdots \\
r_{3,1} & r_{3,2} & r_{3,3} & r_{3,4} & \cdots \\
r_{4,1} & r_{4,2} & r_{4,3} & r_{4,4} & \cdots \\
\vdots & \vdots & \vdots & \vdots & \cdots \\
r_{n+1,1} & r_{n+1,2} & r_{n+1,3} & r_{n+1,4} & \cdots
\end{array}$$

where

$$(r_{i,1} \;\; r_{i,2} \;\; \cdots) \equiv (r_{i-2,2} \;\; r_{i-2,3} \;\; \cdots) - \frac{r_{i-2,1}}{r_{i-1,1}}(r_{i-1,2} \;\; r_{i-1,3} \;\; \cdots), \quad (i > 2)$$

(The notation $r_{i,j}$ stands for row i, column j.) Now we have the following test.

Theorem 3. *(***Routh-Hurwitz Test***) All of the roots of the polynomial (1.2) have real parts strictly less than zero if and only if all $n+1$ elements in the first column of the Routh table are nonzero and have the same sign [22].*

Chapter 2

Model Formulation

2.1 The Allee effect

There are different ways using various mathematical methods to express the Allee effect. For instance, a simplest form of continuous growth equation to describe the Allee effect is given by

$$\frac{dx}{dt} = r(1 - \frac{x}{K})(x - m)x,$$

where $-K < m \ll K$, x is the number/density of cancer cells, for instance in this thesis, r is the reproduction rate and K denotes the carrying capacity. Clearly, if $m = 0$, we have the weak Allee effect, and if $m > 0$, it has the strong Allee effect which means the population growth rate decreases if the population size is below the threshold level m and the population will go to extinction.

More and more ecological research suggest that two or more Allee effects generate mechanisms acting simultaneously on a population (Berec [4]). It has been shown in [49] that many forms of Allee effect models are topologically equivalent. Another popular model with Allee effect is in the form of,

$$\frac{dx}{dt} = r(1 - \frac{x}{K})(x - \frac{m+n}{x+n})x, \tag{2.1}$$

where m is the Allee threshold, and the auxiliary parameter n with $n > 0$ and $m > -n$ (Boukal [35], Sabelis [15], Voorn [25]). It is easy to see that equation (2.1) can be

rewritten as

$$\frac{dx}{dt} = \frac{rx}{x+n}(1 - \frac{x}{K})(x - m), \tag{2.2}$$

(2.2) represents two types of Allee effect affecting the same population, one is the factor $x - m$, and m expresses the minimum of viable population, another is $\frac{rx}{x+n}$ which can be interpreted as the impact of Allee effect due to other causes affecting growth rate, for instance, the predation reducing breeding success at low densities (Clark [36], Gascoigne [30]).

2.2 The Model

Based on the study of the above research, in this thesis, we propose a two-dimensional Ordinary Differential Equation model for the interaction of tumor cells and immune effector cells to study the dynamic behavior and explore the influence of Allee effect on cancer cells and immune effector cells. Immune effector cells here means killer T cells. The basic modeling idea is that we assume immune effector cells attack tumor cells and their proliferation is stimulated, in turn, by the presence of tumor cells.

A general model system is described by the following differential equations,

$$\begin{cases} \dot{x} = r_1 x(1 - \frac{x}{k_1})(1 - \frac{A_1+a_1}{x+a_1}) - \alpha(x)y - \theta(t)x, \\ \dot{y} = r_2 y(1 - \frac{y}{k_2})(1 - \frac{A_2+a_2}{y+a_2}) + \alpha(x)y, \end{cases} \tag{2.3}$$

where $(x, y) \in \Omega = \{(x, y) \in R^2 | x \geqslant 0, y \geqslant 0\}$. $x(t)$ and $y(t)$ denote tumor cells and immune effector cells, respectively, as functions of time t. We describe each equation and all parameters in the following.

For the equation

$$\dot{x} = r_1 x(1 - \frac{x}{k_1})(1 - \frac{A_1 + a_1}{x + a_1}) - \alpha(x)y - \theta(t)x \tag{2.4}$$

where r_1 scales the growth rate of the tumor cells, k_1 is intrinsic carrying capacity, A_1 is the Allee threshold, a_1 is the auxiliary parameters with $a_1 > 0$ and $A_1 > -a_1$. Interaction with immune effector cells and using chemotherapy would lead to the death of cancer cells, which are expressed as $-\alpha(x)y$ and $-\theta(t)x$.

(2.4) can be rewritten as

$$\dot{x} = \frac{r_1 x}{x + a_1}(1 - \frac{x}{k_1})(x - A_1) - \alpha(x)y - \theta(t)x, \tag{2.5}$$

We state that (2.5) represents two types of Allee effect affecting the same population. Clearly, if $A_1 > 0$, we have strong Allee effect. If $A_1 = 0$, it has weak Allee effect.

For the equation

$$\dot{y} = r_2 y(1 - \frac{y}{k_2})(1 - \frac{A_2 + a_2}{y + a_2}) + \alpha(x)y \tag{2.6}$$

where r_2 denotes the growth rate, k_2 is intrinsic carrying capacity, A_2 is the Allee threshold, a_2 is the auxiliary parameters with $a_2 > 0$ and $A_2 > -a_2$. To describe that the presence of cancer cells would stimulate rate of the immune effector cells due to their interaction with tumor cells, we use the term $\alpha(x)y$. Similar to equation (2.5), there are double Allee effects in (2.6) and it must fulfill $-k_i < A_i \ll k_i$ with $i = 1, 2$.

The functional response between the tumor cells and immune effector cells $\alpha(x)$ can be chosen as one of normal Holling type function as the linear $\alpha(x) = px$, hyperbolic $\alpha(x) = \frac{px}{c_0 + x}$ and sigmoid $\alpha(x) = \frac{px^2}{c_0^2 + x^2}$. In order to simplify the analysis of system (2.3), we consider linear functional response $\alpha(x) = px$. The influence of immunotherapy function $\theta(t)$ results a non-autonomous system in general, while we take it as positive constant function for simplicity, $\theta(t) = g_1 > 0$. Therefore through the entire thesis, we mainly work on the following model

$$\begin{cases} \dot{x} = r_1 x(1 - \frac{x}{k_1})(1 - \frac{A_1 + a_1}{x + a_1}) - pxy - g_1 x, \\ \dot{y} = r_2 y(1 - \frac{y}{k_2})(1 - \frac{A_2 + a_2}{y + a_2}) + pxy, \end{cases} \tag{2.7}$$

In order to simplify the analysis of system (2.7), we consider a C^∞-equivalent polynomial extension by the following change of coordinates:

$\phi : \tilde{\Omega} \times R^+ \to \Omega \times R^+$ such that $\phi(u, v, \tau) = \big(k_1 u, k_2 v, (v + \frac{a_2}{k_2})(u + \frac{a_1}{k_1})\tau\big) = (x, y, t)$, with $\tilde{\Omega} = \{(u, v) \in R^2 | u \geqslant 0, v \geqslant 0\}$.

Clearly, the Jacobian determinant: $D\phi(u, v, \tau) = k_1 k_2 (v + \frac{a_2}{k_2})(u + \frac{a_1}{k_1}) > 0$. Then, ϕ is a diffeomorphism preserving the orientation of time and the system (2.7) in the

new system of coordinates is topologically equivalent to the following system (2.8).

$$\begin{cases} \dot{u} = u(v + \frac{a_2}{k_2})[r_1(1-u)(u - \frac{A_1}{k_1}) - g_1(u + \frac{a_1}{k_1}) - pk_2(u + \frac{a_1}{k_1})v] := f_1(u, v), \\ \dot{v} = v(u + \frac{a_1}{k_1})[r_2(1-v)(v - \frac{A_2}{k_2}) + pk_1(v + \frac{a_2}{k_2})u] := f_2(u, v), \end{cases} \tag{2.8}$$

where $\dot{u}, \dot{v}$ denotes $\frac{du}{d\tau}$ and $\frac{dv}{d\tau}$ respectively.

2.3 Positivity and Boundedness

First, we show that the solutions of model (2.7) are nonnegative and bounded. This well-posedness property implies that the proposed model is sensible.

Theorem 4. *The nonnegative orthant R^2_+ is positively invariant under the flow induced by the system (2.7).*

Proof. From the first equation of (2.7), we know that

$$x(t) = x(0)e^{\int_0^t [r_1(1-\frac{x}{k_1})(1-\frac{A_1+a_1}{x+a_1}) - py - g_1]}$$

which means $x(t) > 0$ if and only if $x(0) > 0$. The initial value indicates the positivity of $x(t)$. Similarly, we can obtain the positivity of $y(t)$. This implies that all solutions of the system (2.7) with initial condition $(x(0), y(0)) \in R^2_+$ stays in the first quadrant. □

Theorem 5. *Solutions of model (2.7) are nonnegative and bounded with*

$$\lim_{t\to\infty} sup(x(t) + y(t)) \leq \frac{r_1 k_1}{4g_1} + \frac{k_2}{4r_2 g_1}(r_2 + g_1)^2$$

for $t > 0$.

Proof. For the boundedness of the solution, we define $B(t) = x(t) + y(t)$ and $B(0) = x(0) + y(0) \geq 0$.

Differentiating $B(t)$ with respect to time along the solution of (2.7) yields

$$\begin{aligned} \frac{dB(t)}{dt} &= r_1 x(1 - \frac{x}{k_1})(1 - \frac{A_1 + a_1}{x + a_1}) + r_2 y(1 - \frac{y}{k_2})(1 - \frac{A_2 + a_2}{y + a_2}) - g_1 x \\ &\leq r_1 x(1 - \frac{x}{k_1}) - g_1 x + r_2 y(1 - \frac{y}{k_2}) \end{aligned}$$

Let us consider the following function:

$$\begin{aligned}\frac{dB(t)}{dt}+g_1B(t) &\leq r_1x(1-\frac{x}{k_1})+r_2y(1-\frac{y}{k_2})+g_1y\\ &\leq \frac{r_1k_1}{4}+\frac{k_2}{4r_2}(r_2+g_1)^2\end{aligned}$$

Then, we know

$$B(t)\leq B(0)e^{-g_1t}+(\frac{r_1k_1}{4g_1}+\frac{k_2}{4r_2g_1}(r_2+g_1)^2)(1-e^{-g_1t})$$

when time $t\to\infty$, we have $B(t)\leq \frac{r_1k_1}{4g_1}+\frac{k_2}{4r_2g_1}(r_2+g_1)^2$. This shows that, the solution of system (2.7) is bounded. □

2.4 Existence of Equilibrium Points

2.4.1 Weak Allee effect

In the following we consider weak Allee effect which is described when $A_i=0$ $(i=1,2)$ and the system (2.8) has the form:

$$\begin{cases}\dot{u}=u(v+\frac{a_2}{k_2})[r_1u(1-u)-g_1(u+\frac{a_1}{k_1})-pk_2(u+\frac{a_1}{k_1})v]:=\varphi_1(u,v),\\ \dot{v}=v(u+\frac{a_1}{k_1})[r_2v(1-v)+pk_1(v+\frac{a_2}{k_2})u]:=\varphi_2(u,v),\end{cases}\tag{2.9}$$

To find all the possible equilibrium point, let the functions $\varphi_1(u,v)=\varphi_2(u,v)=0$, we have the following cases:

I Trivial equilibrium point. Obviously, the trivial equilibrium point $E=(u,v)=(0,0)$ always exists.

II Boundary equilibrium point with $u=0$ and $v>0$,

From (2.9), we have

$$r_2(1-v)v=0$$

so there exists one tumor-free equilibrium points $(0,1)$.

III Boundary Equilibrium point with $u > 0$ and $v = 0$.

From (2.9), we have

$$r_1(1-u)u - g_1(u + \frac{a_1}{k_1}) = 0,$$

which yields

$$r_1u^2 - (r_1 - g_1)u + \frac{a_1g_1}{k_1} = 0. \tag{2.10}$$

When $\triangle = (r_1 - g_1)^2 - 4r_1\frac{a_1g_1}{k_1} > 0$ and $r_1 - g_1 > 0$, that is,

$$(\mathbf{K_1}) \qquad g_1 < L^* = r_1(\sqrt{1 + \frac{a_1}{k_1}} - \sqrt{\frac{a_1}{k_1}})^2, \tag{2.11}$$

there exists two positive roots in (2.10), given in the following form:

$u_1 = \frac{r_1 - g_1 + \sqrt{(r_1-g_1)^2 - 4r_1\frac{a_1g_1}{k_1}}}{2r_1}$ and $u_2 = \frac{r_1 - g_1 - \sqrt{(r_1-g_1)^2 - 4r_1\frac{a_1g_1}{k_1}}}{2r_1}$.

Thus with the condition $(\mathbf{K_1})$: $g_1 < L^*$, there are two different boundary equilibrium point. $E_i = (u_i, 0)$ $(i = 1, 2)$in the system. Notably when $g_1 = L^*$, these two equilibrium points E_i merge into one boundary equilibrium point $E_u = (\frac{r_1 - g_1}{2r_1}, 0)$.

IV Positive equilibrium point with $u > 0$ and $v > 0$:

From (2.9)

$$\begin{cases} r_1(1-u)u - g_1(u + \frac{a_1}{k_1}) - pk_2(u + \frac{a_1}{k_1})v = 0, \\ r_2(1-v)v + pk_1(v + \frac{a_2}{k_2})u = 0, \end{cases} \tag{2.12}$$

we solve u and v which result the following:

$$\begin{cases} u = -\frac{r_2}{pk_1}(\frac{1 + \frac{a_2}{k_2}}{v + \frac{a_2}{k_2}} - 1)v, \\ v = \frac{r_1}{pk_2}(\frac{1 + \frac{a_1}{k_1}}{u + \frac{a_1}{k_1}} - 1)u - \frac{g_1}{pk_2}. \end{cases} \tag{2.13}$$

To simplify the analysis, we let $u+\frac{a_1}{k_1}=U$ and $v+\frac{a_2}{k_2}=V$, then (2.13) becomes

$$\begin{cases} U=-\frac{r_2}{pk_1}(V-F_2)(\frac{G_2}{V}-1)+\frac{a_1}{k_1}:=h_1(V), \\ V=\frac{r_1}{pk_2}(U-F_1)(\frac{G_1}{U}-1)-\frac{g_1}{pk_2}+\frac{a_2}{k_2}:=h_2(U), \end{cases} \tag{2.14}$$

with

$$F_i=\frac{a_i}{k_i}, \qquad G_i=\frac{a_i}{k_i}+1, \qquad i=1,2.$$

To find the positive roots (u^*,v^*) in (2.12) or (2.13), firstly it is straightforward to check that such (u^*,v^*) must lay in the region $u^*\in(0,1)$ and $v^*\in(1,\infty)$ with the assumption $r_1>g_1$. Consequently, the positive roots (U^*,V^*) in (2.14) must stay in the region

$$\{W\}=\{(U,V)|U\in(F_1,G_1),\ V\in(G_2,\infty)\}=(F_1,G_1)\times(G_2,\infty)$$

Next to discuss the possible intersection points between the two curves $U=h_1(V)$ and $V=h_2(U)$ in the region W, we draw a schematic diagram (Figure 2.1) to explore the intersection points of these two curves.

Next we discuss the possible intersection points between the two curves $U=h_1(V)$ and $V=h_2(U)$ in the regions W.

Both $h_1(V)$ and $h_2(U)$ are quadratic functions. It is easy to check that, in regarding the two branches $V=h_1^{-1}(U)$ in the curve $U=h_1(V)$, as the increasing of U, V is strictly decreasing when $V<\sqrt{F_2G_2}$ and strictly increasing when $V>\sqrt{F_2G_2}$, from $\frac{dV}{dU}=\frac{1}{h_1'(V)}=\frac{pk_1}{r_2(1-\frac{F_2G_2}{V^2})}$.

Thus, the intersection points of h_i for $i=1,2$ can be located from the maximum value of $V=h_2(U)$ with respect to the curve $U=h_1(V)$ in the region W.

Obviously $V=h_2(U)$ reaches its maximum $V_m=\frac{a_2}{k_2}-\frac{g_1}{pk_2}+\frac{r_1}{pk_2}(\sqrt{G_1}-\sqrt{F_1})^2$ at $U_m=\sqrt{F_1G_1}\in(F_1,G_1)$.

Parallely, at $U_m=\sqrt{F_1G_1}$, there are two corresponding points $(U_m,S_\pm)$ on $U=h_1(V)$ with

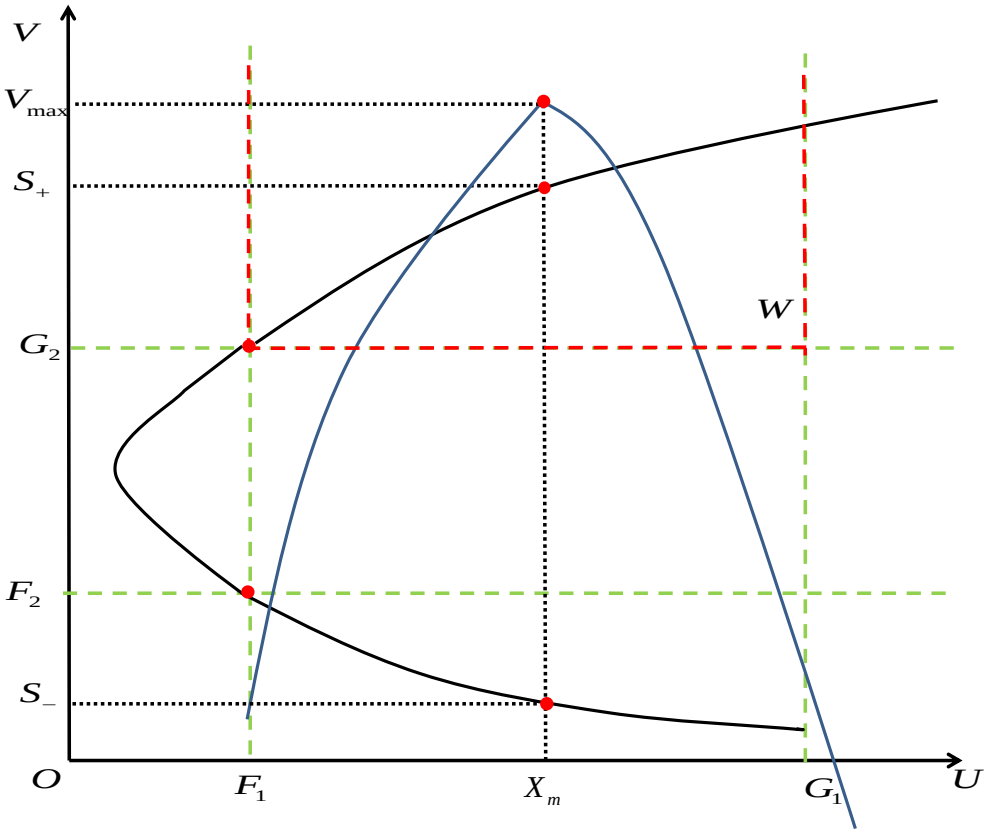

Figure 2.1: Schematic diagram for the intersection of the two curves $U = h_1(V)$ and $V = h_2(U)$. The solid black and blue curve are $h_1(V)$ and $h_2(U)$, respectively.

$$S_{\pm} = \frac{F_2 + G_2 + \frac{pk_1}{r_2}(\sqrt{F_1 G_1} - \frac{a_1}{k_1}) \pm \sqrt{[F_2 + G_2 + \frac{pk_1}{r_2}(\sqrt{F_1 G_1} - \frac{a_1}{k_1})]^2 - 4F_2 G_2}}{2},$$

where $S_- < F_2 < G_2 < S_+$ from

$$h_1(\sqrt{F_2 G_2}) < h_1(F_2) = h_1(G_2) = F_1 < U_m = h_1(S_-) = h_1(S_+)$$

and the monotonicity of $h_1(V)$.

To better discuss and analyze the existence and number of positive equilibrium points in W, we distinct the two cases with the following assumptions:

$$(\mathbf{K_2}): \quad V_m = S_+ \qquad (\mathbf{K_3}): \quad V_m > S_+$$

It should be clear that if $(\mathbf{K_2})$ or $(\mathbf{K_3})$ holds, condition $(\mathbf{K_1})$ holds. In fact, since the intersection points of $h_1(V)$ and $h_2(U)$ stay in the region W, we have $G_2 < V_m$, that is

$$\begin{aligned} \frac{a_2}{k_2} + 1 &< \frac{a_2}{k_2} - \frac{g_1}{pk_2} + \frac{r_1}{pk_2}(\sqrt{G_1} - \sqrt{F_1})^2, \\ g_1 &< r_1(\sqrt{G_1} - \sqrt{F_1})^2 - pk_2. \end{aligned}$$

Clearly, $r_1(\sqrt{G_1} - \sqrt{F_1})^2 - pk_2 < L^*$. Therefore, whether $(\mathbf{K_2})$ or $(\mathbf{K_3})$ holds, $(\mathbf{K_1})$ holds. This implies there are two immune effector-free boundary equilibrium points $E_i = (u_i, 0)$ with $i = 1, 2$.

Then we have the following theorem:

Theorem 6. (**i**) *If condition* $(\mathbf{K_2})$ *hold, there exists a positive equilibrium point in system (2.9).*

(**ii**) *If* $(\mathbf{K_3})$ *hold, there exists two positive equilibrium points in system (2.9).*

We summarize all the possible cases of the number of the equilibrium points in the model and the corresponding conditions in Table 2.1, under the weak Allee effect hypothesis.

Table 2.1: Stationary states in the model with weak Allee effect

Equilibrium	No. E.P.	Existence condition
$E(0,0)$		Always exist
$E(0,1)$		Always exist
$E_1(u_1,0)$		$(\mathbf{K_1})$
$E_2(u_2,0)$		$(\mathbf{K_1})$
$E^*(u^*,v^*)$	1	$(\mathbf{K_2})$
$E^*(u^*,v^*)$	2	$(\mathbf{K_3})$

2.4.2 Strong Allee effect

Strong Allee effect on both tumor cells and immune effector cells implies $A_i > 0$ $(i = 1, 2)$.

Similar to the discussion in the weak Allee effect case, parallely,

I Trivial equilibrium point. Obviously, the trivial E.P. $E_0 = (u, v) = (0, 0)$ always exists.

II Boundary equilibrium point with $u = 0$ and $v > 0$,

From (2.8), we have

$$r_2(1-v)(v-\frac{A_2}{k_2}) = 0$$

so there exists two tumor-free equilibrium points $(0, 1)$ and $(0, \frac{A_2}{k_2})$ which is different from the weak Allee case. The extra steady state $(0, \frac{A_2}{k_2})$ results from the strong Allee effect.

III Boundary Equilibrium point. with $u > 0$ and $v = 0$.

From (2.8), we have

$$r_1(1-u)(u-\frac{A_1}{k_1}) - g_1(u+\frac{a_1}{k_1}) = 0,$$

which yields

$$r_1u^2 - [r_1(1+\frac{A_1}{k_1}) - g_1]u + \frac{r_1A_1 + a_1g_1}{k_1} = 0. \tag{2.15}$$

When $\triangle = [r_1(1+\frac{A_1}{k_1}) - g_1]^2 - 4r_1\frac{r_1A_1+a_1g_1}{k_1} > 0$ and $r_1(1+\frac{A_1}{k_1}) - g_1 > 0$, that is,

$$(\mathbf{H_1}) \qquad g_1 < C^* = r_1(\sqrt{1+\frac{a_1}{k_1}} - \sqrt{\frac{A_1+a_1}{k_1}})^2, \tag{2.16}$$

there exists two boundary positive roots in (2.15), given in the following form:

$u_\pm = \frac{r_1(1+\frac{A_1}{k_1})-g_1 \pm \sqrt{[r_1(1+\frac{A_1}{k_1})-g_1]^2 - 4r_1\frac{r_1A_1+a_1g_1}{k_1}}}{2r_1}$ $(i = 1, 2)$.

Thus with the condition $(\mathbf{H_1})$: $g_1 < C^*$, there are two different positive equilibrium point. $E_\pm = (u_\pm, 0)$ in the system. Notably when $g_1 = C^*$, these two equilibrium points $E_\pm$ merge into one positive boundary equilibrium point $E_u = (\frac{r_1(1+\frac{A_1}{k_1})-g_1}{2r_1}, 0)$.

IV Positive equilibrium point with $u > 0$ and $v > 0$:

Although the discussion is parallel to the weak Allee case, with strong Allee, the analysis is much more complicated.

From (2.8)

$$\begin{cases} r_1(1-u)(u-\frac{A_1}{k_1}) - g_1(u+\frac{a_1}{k_1}) - pk_2(u+\frac{a_1}{k_1})v = 0, \\ r_2(1-v)(v-\frac{A_2}{k_2}) + pk_1(v+\frac{a_2}{k_2})u = 0, \end{cases} \tag{2.17}$$

we solve u and v which result the following:

$$\begin{cases} u = -\frac{r_2}{pk_1}(1+\frac{a_2}{k_2} - (v+\frac{a_2}{k_2}))(1 - \frac{\frac{A_2+a_2}{k_2}}{v+\frac{a_2}{k_2}}), \\ v = \frac{r_1}{pk_2}(1+\frac{a_1}{k_1} - (u+\frac{a_1}{k_1}))(1 - \frac{\frac{A_1+a_1}{k_1}}{u+\frac{a_1}{k_1}}) - \frac{g_1}{pk_2}. \end{cases} \tag{2.18}$$

To simplify the analysis, we let $u+\frac{a_1}{k_1} = X$ and $v+\frac{a_2}{k_2} = Y$, then (2.18) becomes

$$\begin{cases} X = -\frac{r_2}{pk_1}(C_2 - Y)(1-\frac{B_2}{Y}) + \frac{a_1}{k_1} := h_1(Y), \\ Y = \frac{r_1}{pk_2}(C_1 - X)(1-\frac{B_1}{X}) - \frac{g_1}{pk_2} + \frac{a_2}{k_2} := h_2(X), \end{cases} \tag{2.19}$$

with

$$B_i = \frac{A_i + a_i}{k_i}, \qquad C_i = \frac{a_i}{k_i} + 1, \qquad i = 1, 2.$$

Obviously, $0 < C_i - 1 < B_i < C_i$ since $A_i < k_i$ for $i = 1, 2$.

To find the positive roots (u^*, v^*) in (2.17) or (2.18), firstly we can check that such (u^*, v^*) must lay in the region $u^* \in (\frac{A_1}{k_1}, 1)$ and $v^* \in (0, \frac{A_2}{k_2}) \bigcup (1, \infty)$. Different again from the weak Allee case, there is an additional region $(0, \frac{A_2}{k_2})$ for the immune effector cells which can stay in its steady state.

Consequently, the positive roots (X^*, Y^*) in (2.19) must stay in the region

$$D = \{(X, Y) | X \in (B_1, C_1),\ Y \in (C_2 - 1, B_2) \cup (C_2, \infty)\} = \{W_1, W_2\}$$

with the two subregions $W_1 = (B_1, C_1) \times (C_2 - 1, B_2)$ and $W_2 = (B_1, C_1) \times (C_2, \infty)$.

Next we discuss the possible intersection points between the two curves $X = h_1(Y)$ and $Y = h_2(X)$ in the regions W_1 and W_2. (See Figure 2.2).

Parallel to the previous discuss, we know that the intersection points of h_i for $i = 1, 2$ can be located corresponding to the maximum value of $Y = h_2(X)$ with respect to the curve $X = h_1(Y)$ in the regions W_1 and W_2.

Since $Y = h_2(X)$ reaches its maximum $Y_m = \frac{a_2}{k_2} - \frac{g_1}{pk_2} + \frac{r_1}{pk_2}(\sqrt{C_1} - \sqrt{B_1})^2$ at $X_m = \sqrt{B_1 C_1} \in (B_1, C_1)$. If the intersection points exist in W_1, then $Y_m > C_2 - 1$ which implies the condition $(\mathbf{H_1}):\ g_1 < C^*$ exactly. While at $\hat{Y} = C_2 - 1$, there are two points $(M_\pm, \hat{Y})$ on the curve $Y = h_2(X)$ with

$$M_\pm = \frac{B_1 + C_1 - \frac{g_1}{r_1} \pm \sqrt{(B_1 + C_1 - \frac{g_1}{r_1})^2 - 4B_1 C_1}}{2} \in (B_1, C_1). \tag{2.20}$$

In fact, on the curve $Y = h_2(X)$, from $\frac{dY}{dX} = h_2'(X) = \frac{r_1}{pk_2}(\frac{B_1 C_1}{X^2} - 1)$, we know $Y = h_2(X)$ is strictly increasing when $X < X_m = \sqrt{B_1 C_1}$ and strictly decreasing when $X > X_m$, and

$$h_2(B_1) = h_2(C_1) = \hat{Y} - \frac{g_1}{pk_2} < \hat{Y} = h_2(M_-) = h_2(M_+) < Y_m,$$

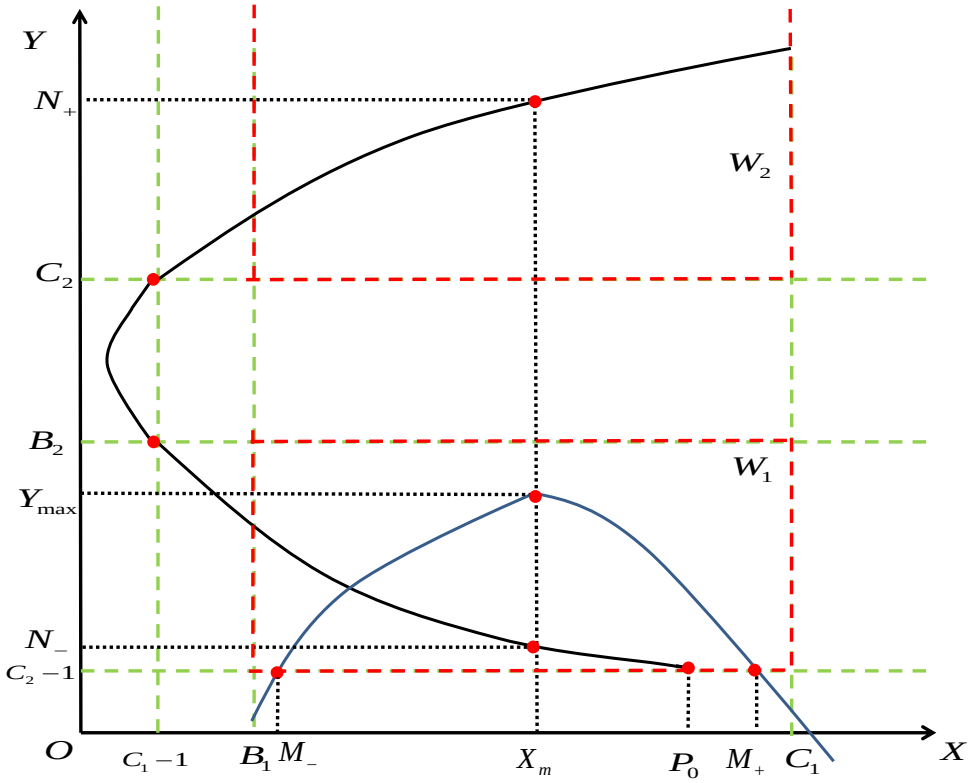

Figure 2.2: Schematic diagram for the intersection of the two curves $X = h_1(Y)$ and $Y = h_2(X)$.

thus $B_1 < M_- < X_m < M_+ < C_1$.

Similarly, at $X_m = \sqrt{B_1C_1}$, there are two corresponding points $(X_m, N_\pm)$ on $X = h_1(Y)$ with

$$N_\pm = \frac{B_2 + C_2 + \frac{pk_1}{r_2}(\sqrt{B_1C_1} - \frac{a_1}{k_1}) \pm \sqrt{[B_2 + C_2 + \frac{pk_1}{r_2}(\sqrt{B_1C_1} - \frac{a_1}{k_1})]^2 - 4B_2C_2}}{2}, \tag{2.21}$$

where $N_- < B_2 < C_2 < N_+$ from $h_1(\sqrt{B_2C_2}) < h_1(B_2) = h_1(C_2) = C_1 - 1 < X_m = h_1(N_-) = h_1(N_+)$ and the monotonicity of $h_1(Y)$.

On the other side, there is one point $(P_0, \hat{Y})$ on the curve $X = h_1(Y)$ with

$$P_0 = h_1(C_2 - 1) = \frac{a_1}{k_1} + \frac{r_2}{pk_1}\frac{A_2}{a_2}. \tag{2.22}$$

Therefore if and only if

$$(\mathbf{H_2}) : P_0 > M_-,$$

there is at least one intersection point in W_1. More specifically, if $P_0 > X_m$, that is $h_1(N_-) = X_m < P_0 = h_1(C_2 - 1)$ in W_1, then $N_- > C_2 - 1$.

With different relation of the values among P_0, M_+, Y_m and $N_\pm$, we can identity the exact numbers of positive equilibrium points. Notably we make the following assumptions:

$$\begin{array}{lll} (\mathbf{H_3}) : \quad P_0 < M_+ & (\mathbf{H_4}) : \quad Y_m < N_+ & (\mathbf{H_5}) : \quad Y_m > N_- \\ (\mathbf{H_6}) : \quad P_0 > M_+ & (\mathbf{H_7}) : \quad Y_m = N_+ & (\mathbf{H_8}) : \quad Y_m > N_+ \end{array}$$

It should be noted that if $(\mathbf{H_5})$, $(\mathbf{H_7})$ or $(\mathbf{H_8})$ holds, condition $(\mathbf{H_1})$ holds. In fact, since the intersection points of $h_1(Y)$ and $h_2(X)$ stay in the region $W_1 \cup W_2$, we have $C_2 - 1 < Y_m$, that is

$$\begin{aligned} \frac{a_2}{k_2} + 1 - 1 &< \frac{a_2}{k_2} - \frac{g_1}{pk_2} + \frac{r_1}{pk_2}(\sqrt{C_1} - \sqrt{B_1})^2, \\ g_1 &< r_1(\sqrt{C_1} - \sqrt{B_1})^2 = C^*. \end{aligned}$$

Therefore, we have the following theorem:

Theorem 7. (**i**) *If* $(\mathbf{H_1}) \sim (\mathbf{H_4})$ *hold, there exists a positive equilibrium point in system (2.8).*

(**ii**) *If either* $(\mathbf{H_4}) \sim (\mathbf{H_6})$, *or* $(\mathbf{H_2}) \sim (\mathbf{H_3})$ *and* $(\mathbf{H_7})$, *hold, there exists two positive equilibrium points in system (2.8).*

(**iii**) *If either* $(\mathbf{H_6}) \sim (\mathbf{H_7})$, *or* $(\mathbf{H_2}) \sim (\mathbf{H_3})$ *and* $(\mathbf{H_8})$, *holds, there exists three positive equilibrium points in system (2.8).*

(**iv**) *If* $(\mathbf{H_6})$ *and* $(\mathbf{H_8})$ *holds, there exists four positive equilibrium points in system (2.8).*

The results of the number of the Equilibrium points of the model and the associated conditions are summarized in Table 2.2.

Table 2.2: Stationary states in the model with strong Allee effect

Equilibrium	No. E.P.	Existence condition
$E_0(0,0)$		Always exist
$E_{01}(0,\frac{A_2}{k_2})$		Always exist
$E_{02}(0,1)$		Always exist
$E_+(u_+,0)$		$(\mathbf{H_1})$
$E_-(u_-,0)$		$(\mathbf{H_1})$
$E^*(u^*,v^*)$	1	$(\mathbf{H_1}) \sim (\mathbf{H_4})$
$E^*(u^*,v^*)$	2	$(\mathbf{H_4}) \sim (\mathbf{H_6})$
$E^*(u^*,v^*)$	2	$(\mathbf{H_2}) \sim (\mathbf{H_3})$, $(\mathbf{H_7})$
$E^*(u^*,v^*)$	3	$(\mathbf{H_2}) \sim (\mathbf{H_3})$, $(\mathbf{H_8})$
$E^*(u^*,v^*)$	3	$(\mathbf{H_6})$, $(\mathbf{H_7})$
$E^*(u^*,v^*)$	4	$(\mathbf{H_6})$, $(\mathbf{H_8})$

2.5 Stability Analysis

As we know from the preliminaries that the local stability near an hyperbolic equilibrium point can be determined from the characteristic equation of the linearized system.

At each equilibrium point $E = (u^*, v^*)$, the characteristic equation for system (2.8) is

$$\lambda^2 - (\delta_1 + \delta_4)\lambda + \delta_1\delta_4 - \delta_2\delta_3 = 0. \tag{2.23}$$

where

$$\begin{aligned}
\delta_1 &= (v^* + \frac{a_2}{k_2})[r_1(1-u^*)(u^* - \frac{A_1}{k_1}) - (g_1 + pk_2v^*)(2u^* + \frac{a_1}{k_1}) + r_1u^*(1 + \frac{A_1}{k_1} - 2u^*)],\\
\delta_2 &= u^*[r_1(1-u^*)(u^* - \frac{A_1}{k_1}) - g_1(u^* + \frac{a_1}{k_1}) - pk_2(u^* + \frac{a_1}{k_1})(2v^* + \frac{a_2}{k_2})],\\
\delta_3 &= v^*[r_2(1-v^*)(v^* - \frac{A_2}{k_2}) + pk_1(v^* + \frac{a_2}{k_2})(2u^* + \frac{a_1}{k_1})],\\
\delta_4 &= (u^* + \frac{a_1}{k_1})[r_2(1-v^*)(v^* - \frac{A_2}{k_2}) + pk_1u^*(2v^* + \frac{a_2}{k_2}) + r_2v^*(1 + \frac{A_2}{k_2} - 2v^*)].
\end{aligned}$$

Therefore, we can obtain the stability conditions for the trivial/boundary equilibrium

points in a straightforward way. Although we have provided the existence conditions for the positive equilibrium points previously, due to the complexity of the system, it is impossible to discuss the stabilities of those steady states explicitly. We will provide some numerical simulations to display their rich dynamics.

Theorem 8. *For the Weak Allee Effect case ($A_i = 0$),*

(**i**) *$E(0,1)$ is always locally asymptotically stable.*

(**ii**) *$E_1(u_1, 0)$ is saddle point; and $E_2(u_2, 0)$ is unstable point.*

(**iii**) *The point $E(0,0)$ is a non-hyperbolic singularity.*

Proof. (**i**) The characteristic equation of (2.9) at $E(0,1)$ is

$$(\lambda_1 + (\frac{a_2}{k_2} + 1)\frac{g_1 a_1 + pk_2 a_1}{k_1})(\lambda_2 + r_2\frac{a_1}{k_1}) = 0$$

Obviously both λ_1 and λ_2 are negative since all the paramters are positive. Therefore, $E(0,1)$ is always locally asymptotically stable.

(**ii**) At $E_i(u_i, 0)$ $(i = 1, 2)$, (2.23) becomes

$$(\lambda_{1i} - u_i \cdot \frac{a_2}{k_2}[r_1 - 2r_1 u_i - g_1])(\lambda_{2i} - u_i k_1 p\frac{a_2}{k_2}(u_i + \frac{a_1}{k_1})) = 0,$$

It is easy to see that both E_i are unstable from

$$\lambda_{2i} = u_i k_1 p\frac{a_2}{k_2}(u_i + \frac{a_1}{k_1}) > 0.$$

More specifically, recall that, $E_i(u_i, 0)$ exists under the condition given in ($\mathbf{K_1}$), with

$$0 < u_2 < \frac{r_1 - g_1}{2r_1} < u_1.$$

From

$$\lambda_{11} = u_1 \cdot \frac{a_2}{k_2}[r_1 - 2r_1 u_1 - g_1] = u_1 \cdot \frac{a_2}{k_2} 2r_1(\frac{r_1 - g_1}{2r_1} - u_1) < 0,$$

$$\lambda_{12} = u_2\frac{a_2}{k_2}[r_1 - 2r_1 u_2 - g_1] = u_2 \cdot \frac{a_2}{k_2} 2r_1(\frac{r_1 - g_1}{2r_1} - u_2) > 0,$$

we know that $E_1(u_1, 0)$ is unstable saddle node and $E_2(u_2, 0)$ is a unstable node.

(iii) The characteristic equation of (2.9) at $E(0,0)$ is

$$\lambda_1(\lambda_2 + g_1\frac{a_1a_2}{k_1k_2}) = 0$$

$\lambda_1 = 0$ which implies we can not obtain its local stability by computing eigenvalues and $E(0,0)$ is non-hyperbolic singularity. □

Theorem 9. *For Strong Allee Effect case ($A_i > 0$),*

(**i**) $E_0(0,0)$ *is always locally asymptotically stable.*

(**ii**) $E_{01}(0, \frac{A_2}{k_2})$ *is always an unstable saddle point; $E_{02}(0,1)$ is always locally asymptotically stable.*

(**iii**) *If $u_+ < \frac{r_2A_2}{pk_1a_2}$, then $E_+(u_+,0)$ is stable and $E_-(u_-,0)$ is saddle point; If $u_- < \frac{r_2A_2}{pk_1a_2} < u_+$, then $E_+(u_+,0)$ and $E_-(u_-,0)$ are saddle point; If $\frac{r_2A_2}{pk_1a_2} < u_- < u_+$, then $E_+(u_+,0)$ is saddle point and $E_-(u_-,0)$ is unstable node.(See Table 2.3)*

Proof. (**i**) it is straightforward to show that the characteristic equation of (2.9) at $E_0(0,0)$ is

$$\big(\lambda + \frac{a_2(r_1A_1 + g_1a_1)}{k_1k_2}\big)\big(\lambda + \frac{a_1r_2A_2}{k_1k_2}\big) = 0$$

So it is easy to obtain that $E_0(0,0)$ is always stable.

(**ii**) The characteristic equation of (2.8) at $E_{01}(0, \frac{A_2}{k_2})$ and $E_{02}(0,1)$ are, respectively,

$$(\lambda_1 + (a_2 + A_2)\frac{r_1A_1 + g_1a_1 + pA_2a_1}{k_1k_2})(\lambda_2 - r_2\frac{a_1A_2}{k_1k_2}(1 - \frac{A_2}{k_2})) = 0$$

and

$$(\lambda_1 + (\frac{a_2}{k_2} + 1)\frac{r_1A_1 + g_1a_1 + pk_2a_1}{k_1})(\lambda_2 + r_2\frac{a_1}{k_1}(1 - \frac{A_2}{k_2})) = 0.$$

Since $k_2 > A_2$, we know E_{01} is an unstable saddle point and E_{02} is always stable.

(**iii**) The linearization of (2.9) at $E_\pm(u_\pm, 0)$ is given by

$$\begin{cases} u'(t) = u_\pm\frac{a_2}{k_2}[r_1(1 + \frac{A_1}{k_1}) - 2r_1u_\pm - g_1]u(t) - u_\pm pa_2(u_\pm + \frac{a_1}{k_1})v(t), \\ v'(t) = (u_\pm + \frac{a_1}{k_1})(u_\pm k_1p\frac{a_2}{k_2} - r_2\frac{A_2}{k_2})v(t), \end{cases} \tag{2.24}$$

Recall that $E_{\pm}(u_{\pm}, 0)$ exists under the condition $(\mathbf{H_1})$, with

$$0 < u_- < \frac{r_1(1 + \frac{A_1}{k_1}) - g_1}{2r_1} < u_+.$$

Thus for the stability of $E_+(u_+, 0)$, from the characteristic equation of (2.24)

$$(\lambda_{1+} - u_+ \cdot \frac{a_2}{k_2}[r_1(1 + \frac{A_1}{k_1}) - 2r_1u_+ - g_1])(\lambda_{2+} - (u_+ + \frac{a_1}{k_1})(u_+k_1p\frac{a_2}{k_2} - r_2\frac{A_2}{k_2})) = 0,$$

we have

$$\lambda_{1+} = u_+ \cdot \frac{a_2}{k_2}[r_1(1 + \frac{A_1}{k_1}) - 2r_1u_+ - g_1] = u_+ \cdot \frac{a_2}{k_2}2r_1(\frac{r_1(1 + \frac{A_1}{k_1}) - g_1}{2r_1} - u_+) < 0,$$

and

$$\lambda_{2+} = (u_+ + \frac{a_1}{k_1})(u_+k_1p\frac{a_2}{k_2} - r_2\frac{A_2}{k_2}).$$

Consequently we know that $E_+(u_+, 0)$ is locally asymptotically stable when $u_+ < \frac{r_2A_2}{pk_1a_2}$. Otherwise $E_+(u_+, 0)$ becomes unstable saddle.

In a parallel way, we can show that if $u_- > \frac{r_2A_2}{pk_1a_2}$, $E_-(u_-, 0)$ is a unstable node; if not, $E_-(u_-, 0)$ is a unstable saddle node.

In short, we can conclude that the stability conditions of the equilibrium points of E_+ and E_- in the following table.

Table 2.3: Stability of $E_+(u_+, 0)$ and $E_-(u_-, 0)$

	$E_+(u_+, 0)$	$E_-(u_-, 0)$
$u_+ < \frac{r_2A_2}{pk_1a_2}$	locally stable	saddle
$u_- < \frac{r_2A_2}{pk_1a_2} < u_+$	saddle	saddle
$\frac{r_2A_2}{pk_1a_2} < u_-$	saddle	unstable node

□

Chapter 3

Sensitivity Analysis

In this project, the primary model outputs of interest for the sensitivity analyses were the density of cancer cells. Therefore, we choose the density of cancer cells as the sensitivity function to rank the influential parameters in our model that affect the density of cancer cells . The uncertainty of the model output is generally arose from the uncertainty of inputting parameters. A good technique to assess and address uncertainties is uncertainty analysis (UA).

In the following, we use the most popular sampling-based approach i.e. Latin Hypercube sampling (LHS) to perform uncertainty analysis (McKay [38], Jain [13]). LHS is one kind of Monte Carlo sampling methods to determine the uncertainty in model output. It is stratified sampling that provide each random parameter range with an equal probability to sample every parameter. Compared with random sampling, LHS requires fewer samples and a minimum number of computer simulation, but it does not lose its accuracy. It also ensures an unbiased estimate of the average model output. Moreover, if the parameter range is very large, performing a log scale on the parameter range for LHS can prevent under-sampling (Marino [39]). Furthermore, LHS ensures that exactly one parameter is sampled from each stratum in a given sample without replacement.

Using the MATLAB LHS and PRCC code provided in (Marino [39]), we perform sensitivity analyses on all the parameters using PRCC analysis by sampling parameters from a uniformly distributed range using LHS. Here, the parameters is sampled 40 time for 40 runs. All the parameter values (except the auxiliary parameters α_i for cancer/immune effector cells) are chosen from references, see Table 4.1.

We can see the relationship between the density of cancer cells and input parameters from scatter plots, along with PRCC values and p-values. This has been shown in Figure 3.1. Parameters with large PRCC values (> 0.5, or $<$ -0.5) as well as corresponding small p-values (< 0.05) are the most important (Richard [16]). If the PRCC value is closer to $+1$ or -1, the LHS parameters has more strongly impact on the outcome. The sign implies the relationship between the input parameters and output variable.

We have also done the uncertainty and sensitivity analysis with each parameters, see Figure 3.2. The PRCC between the density of cancer cells and each parameters in Figure 3.2, indicates the expected number the cancer cells has a significantly positive relation with A_1. This is reasonable because A_1 is the threshold, below which the population size decreases or insreases when the parameter is below or above the threshold value. In addition, we notice that A_1 has higher PRCC values than other the parameters. Thus, A_1 is the most influential parameter on the density of cancer cells.

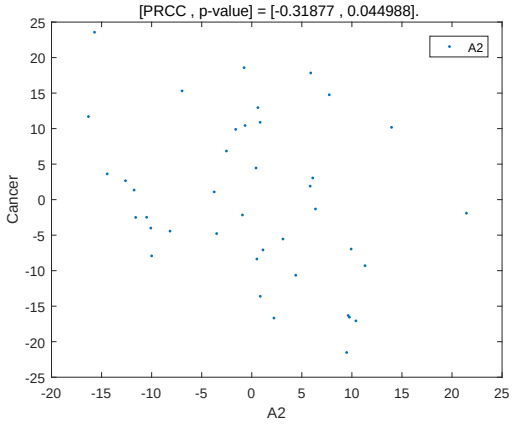
[PRCC , p-value] = [-0.31877 , 0.044988].
A2
Cancer
A2

(a)

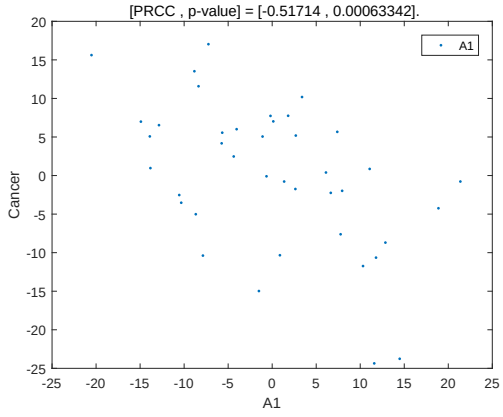
[PRCC , p-value] = [-0.51714 , 0.00063342].
A1
Cancer
A1

(b)

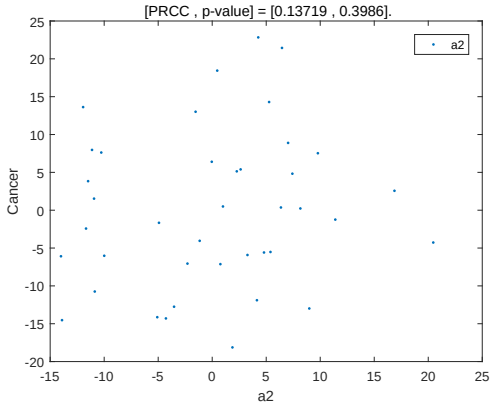
[PRCC , p-value] = [0.13719 , 0.3986].
a2
Cancer
a2

(c)

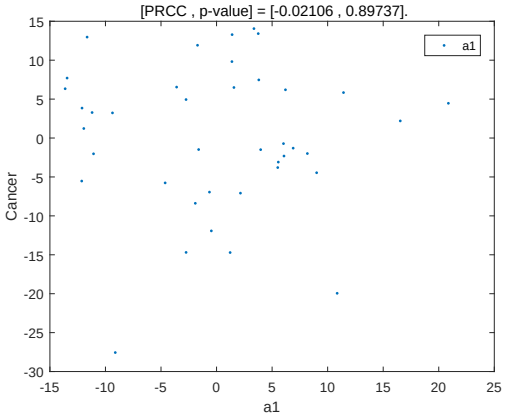
[PRCC , p-value] = [-0.02106 , 0.89737].
a1
Cancer
a1

(d)

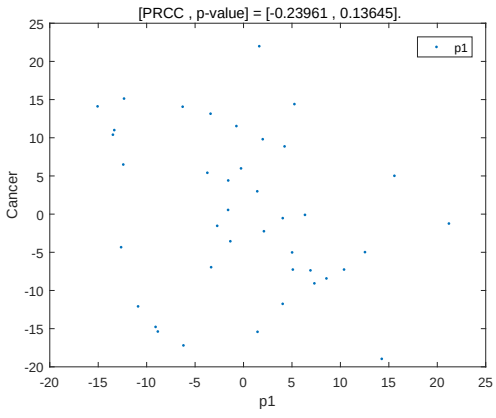
[PRCC , p-value] = [-0.23961 , 0.13645].
p1
Cancer
p1

(e)

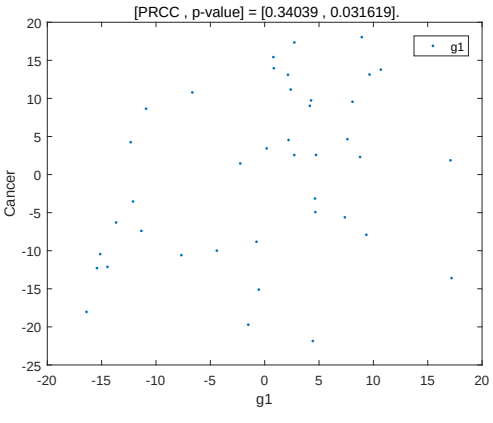
[PRCC , p-value] = [0.34039 , 0.031619].
g1
Cancer
g1

(f)

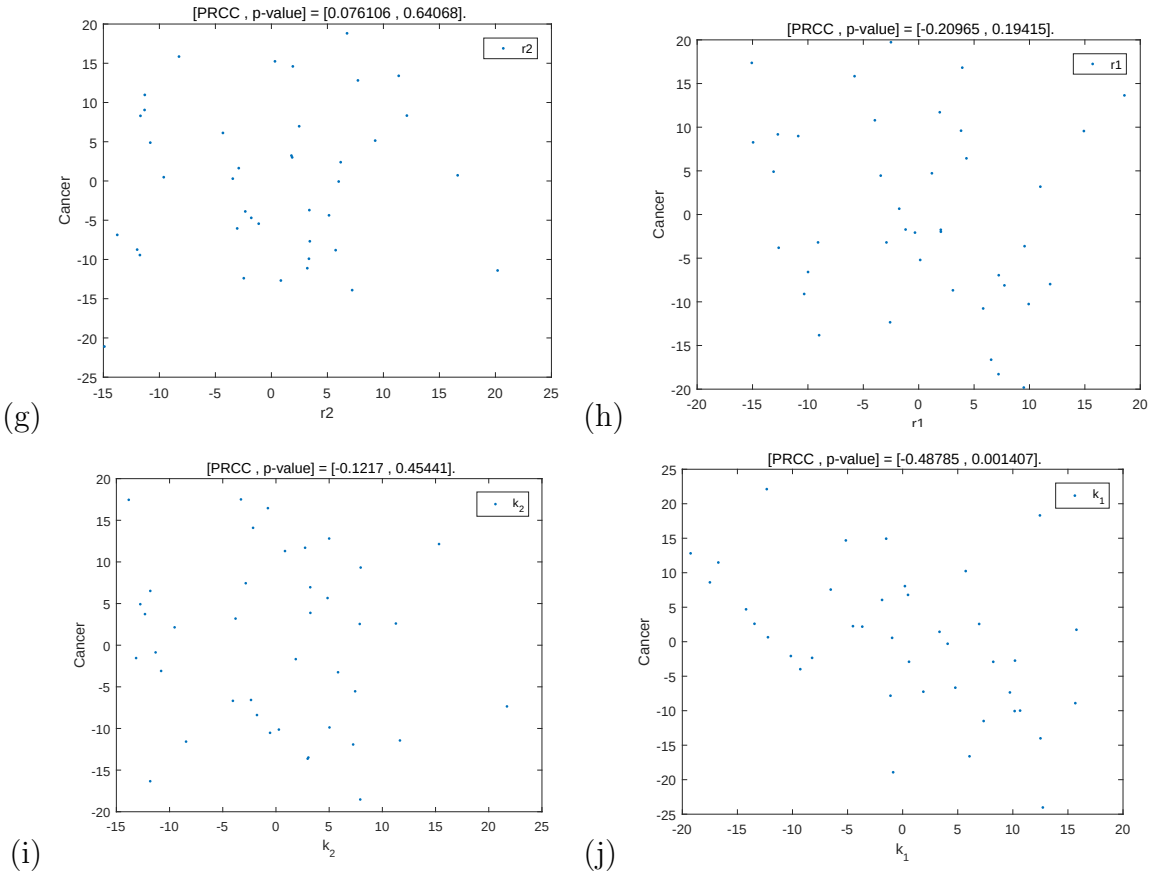

Figure 3.1: Scatter plots showing either monotonic relationships or no relationships between input parameters and cancer cells. p-values that are greater than 0.05 are not statistically significant.

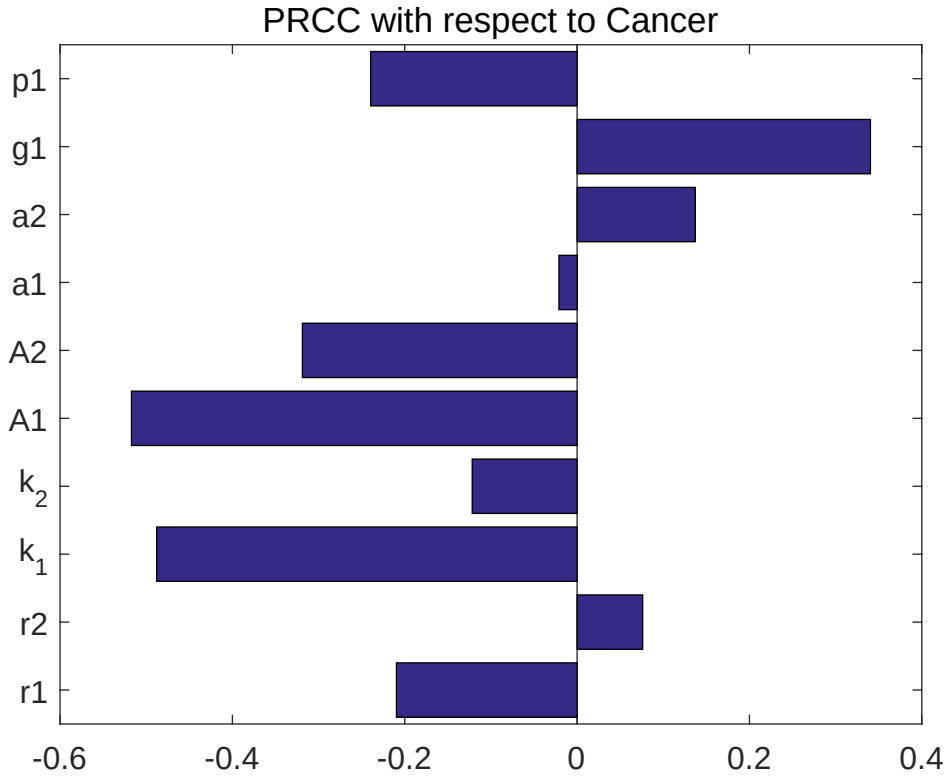

Figure 3.2: PRCC values for Cancer cells under the variation of parameters.

Chapter 4

Numerical Simulation

To make up the lack of theoretical analysis for the positive equilibrium points, in this part, we present some numerical results for Strong Allee Effect case by choosing parameters from Table 4.1.

Case (1) : first we choose

$$r_1 = 4.1; k_1 = 2.764 \times 10^9; a_1 = 0.2764 \times 10^7; A_1 = 10^8; p = 3.4 \times 10^{-9};$$
$$r_2 = 0.8; k_2 = 5 \times 10^8; a_2 = 5 \times 10^6; A_2 = 2 \times 10^7; g_1 = 0.21;$$

then, we know that $C^* = 2.6746$ in Eq. (2.16), $Y_m = 1.4598$, $M_+ = 0.9477$ in Eq. (2.20), $N_+ = 3.2991$ in Eq. (2.21) and $P_0 = 0.3415$ in Eq. (2.22). It is obvious that $(\mathbf{H_1}) \sim (\mathbf{H_4})$ hold. Then two curves of Eq. (2.19) has one positive intersection point $(0.03971, 0.03421)$ in W_1, which implies there exists one positive equilibrium point $E^*(0.0387, 0.0242)$ in the system (2.8).

Since condition $(\mathbf{H_1})$ holds, we know boundary equilibrium points $E_-(0.0383, 0)$ and $E_+(0.9467, 0)$ exist and $E_-(0.0383, 0)$ and $E_+(0.9467, 0)$ are unstable saddle points, from Theorem 9 and $0.0383 < \frac{r_2 A_2}{p k_1 a_2} = 0.3405 < 0.9467$.

By computing the eigenvalue at the endemic equilibrium $E^*(0.0387, 0.0242)$, we know it is unstable (see Figure 4.1). Some nearby trajectories approch to the boundary equilibrium point $E(0, 1)$ which is always locally asymptotically stable, some approch to the stable origin, implying that, under such condition, either the cancer cells will be killed by the immune effector cells or both cells will vanish in a long run, from the

Table 4.1: Parameter estimates

Parameter	Description	Unites	Values (Range)	Source
r_1	Cancer Growth rate	day^{-1}	0.01-0.5	[41], [42], [46]
r_2	Effective contact rate	day^{-1}	0.8	[45]
k_1	Carrying capacity of cancer cells	number of cells	$10^9 - 2.764 \times 10^9$	[44], [48], [45]
k_2	Carrying capacity of immune effector cells	number of cells	5×10^8	[45]
A_1	Allee Threshold for cancer cells	-	$10^6 - 10^8$	Estimated
A_2	Allee Threshold for immune effector cells	-	$10^6 - 10^8$	[45]
a_1	Auxiliary parameters for cancer cells	-	2.764×10^6	Estimated
a_2	Auxiliary parameters for immune effector cells	-	5×10^6	Estimated
p	Increase rate in Immune effector cells proliferation or rate at which immune effector cells kill cancer cells	$\text{cells}^{-1}\text{day}^{-1}$	$3.4 \times 10^{-9} - 1 \times 10^{-3}$	[42], [40]
g_1	loss rate of cancer cells due to chemotherapy	-	0.065 ,0.21,0.24 (day^{-1})	[45], [45], [45]

viewpoint of biology.

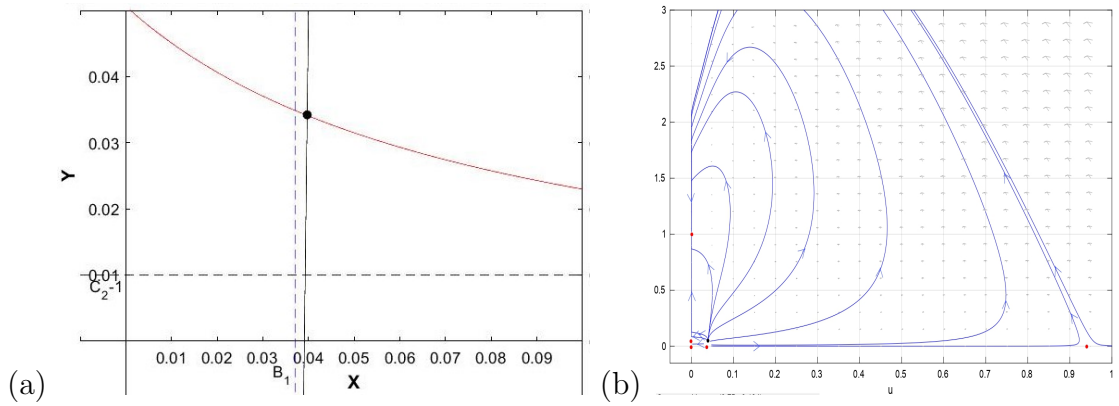

Figure 4.1: The existence of uniqe endemic equilibrium $E^*(0.0387, 0.0242)$ and its stability with $A_1 = 10^8$. (a) Existence of the uniqe equilibrium point (balck spot). (b) Phase portrait.

Case (2) : Based on the data given in **Case (1)**, if we only change the vlue of A_2 to 2×10^8, we obtain $C^* = 2.6764$, $P_0 = 3.4061$, $M_+ = 0.9477$, $Y_m = 1.4598$, $N_- = 0.1164$ and $N_+ = 3.5581$. We can check that $(\mathbf{H_4}) \sim (\mathbf{H_6})$ hold. Then two curves in Eq. (2.19) have two positive intersection points $(0.044, 0.2482)$ and $(0.9375, 0.0335)$ in W_1, implying there exist two positive equilibrium points: $(0.043, 0.238)$ and $(0.9365, 0.0235)$ in the system (2.8), both of them are unstable saddle point. (See Figure 4.2)

Different from that in **Case (1)**, here $0.0383 < 0.9467 < \frac{r_2 A_2}{p k_1 a_2} = 3.4051$, so $E_-(0.0383, 0)$ is saddle point and $E_+(0.9467, 0)$ is stable point, from Theorem 9.

Case (3) : Still keep all the other parameters same as those in **Case (1)**, except for A_1 and $4A_2$. If we change A_2 to 2.5×10^7 and A_1 to 10^7, we have $C^* = 3.5655$, $P_0 = 0.4266$, $M_+ = 0.9495$, $Y_m = 1.9838$, $N_- = 0.0332$ and $N_+ = 1.8237$ and $(\mathbf{H_2}) \sim (\mathbf{H_3})$, and $(\mathbf{H_8})$ hold. Then two curves in Eq. (2.19) have three positive intersection points: one $(0.005, 0.057)$ in W_1, and two $(0.082, 1.978)$, $(0.0095, 1.12)$ in W_2 (see Figure (4.3) (a)). Thus, the system (2.8) have three positive equilibrium points: $(0.004, 0.047)$, $(0.081, 1.97)$,$(0.0085, 1.11)$. By computing the eigenvalue at these equilibrium points, we know that they are unstable node, locally stable spiral, an unstable saddle point, respectively. (See Figure 4.3 (b))

The existence of the boundary equilibrium points and their stabilities are similar

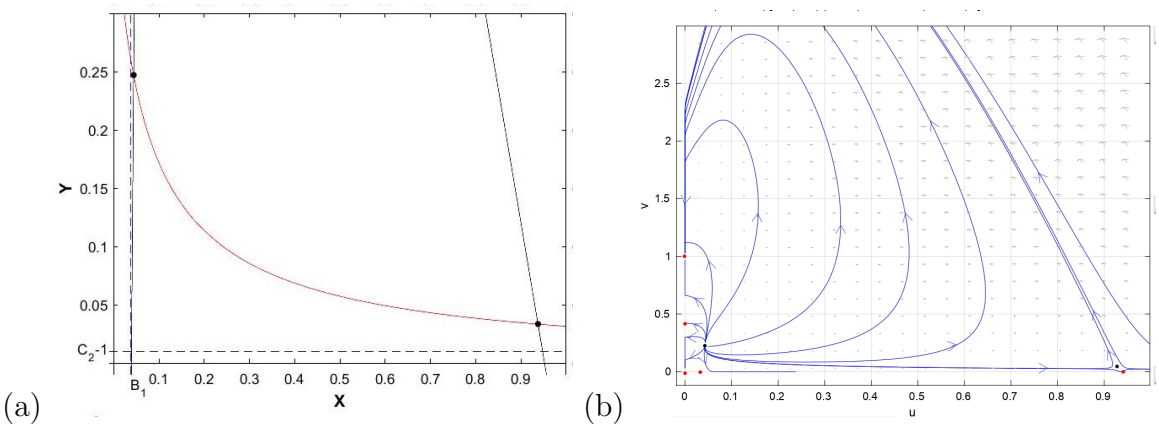

Figure 4.2: The existence of two endemic equilibrium points and their stabilities with $A_1 = 2\times 10^8$. (a) Existence of two equilibrium points (black spot). (b) Phase portrait.

to that in **Case (1)**.

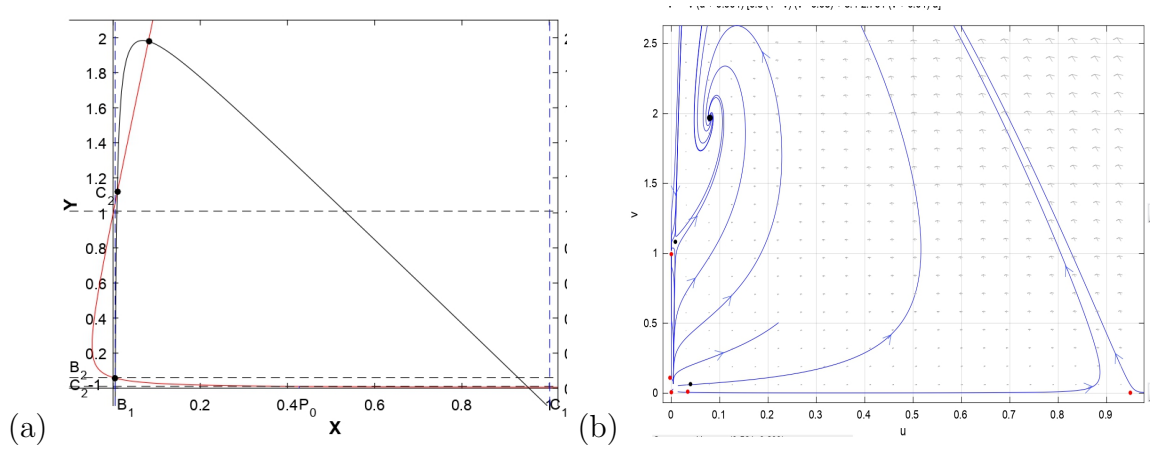

Figure 4.3: (a) Existence of three positive equilibrium points. (b) Phase portrait with $A_2 = 2.5 \times 10^7, A_1 = 10^7$.

Case (4) : Again based on the data in **Case (1)**, when we change A_2 to 2×10^8 and p to 3.4×10^{-10}, then, we have $C^* = 2.6746$, $P_0 = 34.0522$, $M_+ = 0.9477$, $Y_m = 14.5078$, and $N_+ = 1.3353$ and we can check that $(\mathbf{H_6})$ and $(\mathbf{H_8})$ hold. So the two curves in (2.19) have four positive intersection points: $(0.04, 0.382)$ and $(0.94, 0.185)$ in W_1, $(0.041, 1.09)$ and $(0.85, 2.233)$ in W_2. Thus, there exists four positive equilibrium points, and by calculating the eigenvalue at these points, we have the following results:

i Unstable node $(0.039, 0.372)$;

ii Unstable saddle point $(0.939, 0.175)$ and $(0.04, 1.08)$;

iii Locally asymptotically stable $(0.849, 2.223)$.

(See Figure 4.4)

The existence of the boundary equilibrium points and their stabilities are similar to those in **Case (2)**.

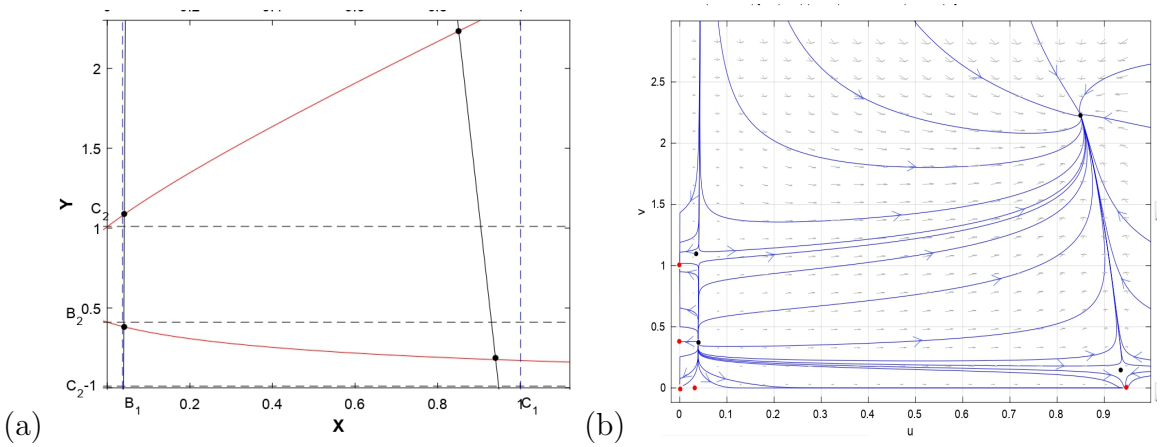

Figure 4.4: (a) Existence of four positive equilibrium points with $A_2 = 2 \times 10^8, p = 3.4 \times 10^{-10}$. (b) Phase portrait.

Chapter 5

Summary and Future Work

In this thesis, we propose a general model to explore the influence of Allee effect on immune effector cells and cancer cells .

In chapter 2, we simplified the general model to discuss the existence of steady states and their local stabilities. For the boundary equilibrium points and trivial equilibrium point under weak/strong Allee effect, we have discussed the existence conditions and all possible numbers of positive equilibrium points, and further provided the explicit conditions for the local stability at the boundary equilibrium points.

In Chapter 3, we use LHS and PRCC methods to analysis the influences of each parameters and confirm that which parameter has a great/least impact on the density of Cancer cells.

In Chapter 4, we illustrate some numerical simulation to show the possibilities of one to four positive equilibrium points and their stabilities.

Although I have done some work for the existence and stability of the equilibrium points in the model 2.8, but no bifrucation analysis has been carried beyond the stability regions. Due to the complexity of the model, there may have different kinds of bifurcations we can investigate.

Further research of this thesis, one would like to change the form of $\alpha(x)$ and $\theta(t)$ in the system 2.8. For instance, the hyperbolic hyperbolic $\alpha(x) = \frac{px}{c_0+x}$ and sigmoid $\alpha(x) = \frac{px^2}{c_0^2+x^2}$, etc. and $\theta(t) = \beta t$ or other complex form. And using Poincaré-Bendixson theorem to analytically study the global dynamics of the model for centain range of parameters in order to gain more biological insights.

Another direction of future work is in introducing time delay. For example, a time delay for the interaction between cancer cells and immune effector cells or time delay for the proliferation of cancer cells and immune effector cells.

Bibliography

[1] F. M. Burnet, Cancer- a biological approach, Brit. Med. J., 1(1957), 841-847.

[2] L. Thomas, Discussion in "Cellular and Humoral Aspects of the Hypersensitive States" (ed. H. S. Lawrence), Hoeber-Harper, New York, 1959, pp. 529-532.

[3] G. P. Dunn, L. J. Old and R. D. Schreiber, The three Es of cancer immunoediting, Annu. Rev. Immunol., 22 (2004), 329-360.

[4] L. Berec, E. Angulo, and F. Courchamp, Multiple Allee effects and population management, Trends Ecology Evol., 22 (2007), pp. 185C191.

[5] G. P. Dunn, A. T. Bruce, H. Ikeda, L. J. Old and R. D. Schreiber, Cancer immunoediting: From immunosurveillance to tumor escape, Nature Immunol., 3 (2002), 991-998.

[6] L. Sewalt, K. Harley, P. van Heijster, et al., Influences of allee effects in the spreading of malignant tumours, J. Theor. Biol., 394 (2016), 77C92.

[7] H. Matsushita, M. D. Vesely, D. C. Koboldt et al., Cancer exome analysis reveals a T-celldependent mechanism of cancer immunoediting, Nature, 482 (2012), 400-404.

[8] F. E. MCKENZIE, W. H. BOSSERT,An integrated model of plasmodium falciparum dynamics, J. theoret. Biol 232, (2005), 411-426.

[9] KIRCHNER D. (1996),Using mathematics to understand HIV immune dynamics, Notice of AMS, vol 43, Number 2,191-202.

[10] V. Kuznetsov, I. Makalkin, M. Taylor, and A. Perelson, Nonlinear dynamics of immunogenic tumors: Parameter estimationestimation and global bifurcation analysis, Bull. Math. Biol., 56 (1994), pp. 295C321.

[11] M. Mohme, S. Riethdorf and K. Pantel, Circulating and disseminated tumour cells - mechanisms of immune surveillance and escape, Nat. Rev. Clin. Oncol., 14 (2017), 155-167.

[12] D. Pardoll, Does the immune system see tumors as foreign or self? Annu. Rev. Immunol.,21 (2003), 807-839.

[13] Jain, Sharad K., and Vijay P. Singh. Water resources systems planning and management. Elsevier, 2003.

[14] D. Kirschner and J. Panetta, Modeling immunotherapy of the tumor-immune interaction, J. Math. Biol., 37 (1998), pp. 235C252.

[15] D. S. Boukal, M. W. Sabelis, L.Berec, How predator functional responses and Allee effects in prey affect the paradox of enrichment and population collapses, Theoretical Population Biology, 72(2007)36-147.

[16] Richard Taylor. Interpretation of the correlation coeffcient: A basic review. Journal of Diagnostic Medical Sonography, 6(1):3539, 1990.

[17] C. M. Koebel, W. Vermi, J. B. Swann, N. Zerafa, S. J. Rodig, L. J. Old, M. J. Smyth and R. D. Schreiber, Adaptive immunity maintains occult cancer in an equilibrium state, Nature,450 (2007), 903-907.

[18] M. D. Vesely, M. H. Kershaw, R. D. Schreiber and M. J. Smyth, Natural innate and adaptive immunity to cancer, Annu. Rev. Immunol., 29 (2011), 235-271.

[19] P. Feng, Z. Dai, D. Wallace, On a 2d model of avascular tumor with weak allee effect, J. Appl. Math., 2019 (2019).

[20] Siegel, R., Miller, K., and Jemal, A. (2015). Cancer statistics, 2015. CA: A Cancer Journal for Clinicians, 65(1), 5C29.

[21] M. Owen and J. Sherratt, Modeling the macrophage invasion of tumors: Effects on growth and composition, Math. Med. Biol., 15 (1998), pp. 165C185.

[22] Wiggins, Stephen, Stephen Wiggins, and Martin Golubitsky. Introduction to applied nonlinear dynamical systems and chaos. Vol. 2. New York: springer-verlag, 1990.

[23] Sterman, John.D. (2000). Business Dynamics Systems Thinking And Modelling In A Complex World, Mcgraw-Hill, New York.

[24] Strogatz, Steven H. Nonlinear dynamics and chaos with student solutions manual: With applications to physics, biology, chemistry, and engineering. CRC press, 2018.

[25] G. A. K. van Voorn, L. Hemerik, M. P. Boer, B. W. Kooi, Heteroclinic orbits indicate overexploitation in predator-prey systems with a strong Allee effect, Mathematical Biosciences 209(2007)451-469.

[26] A. Konstorum, T. Hillen, J. Lowengrub, Feedback regulation in a cancer stem cell model can cause an allee effect, B. Math. Biol., 78 (2016), 754C785.

[27] R. D. Schreiber, L. J. Old and M. J. Smyth, Cancer immunoediting: Integrating immunity's roles in cancer suppression and promotion, Science, 331 (2011), 1565-1570.

[28] Z. Neufeld, W. von Witt, D. Lakatos, et al., The role of allee effect in modelling post resection recurrence of glioblastoma, PLoS Comput. Biol., 13 (2017), e1005818.

[29] World Health Organization (WHO), 3 March 2021, https://www.who.int/news-room/fact-sheets/detail/cancer.

[30] J. Gascoigne and R. N. Lipcius, Allee effects in marine systems, Marine Ecology Prog. Ser., 269 (2004), pp. 49C59.

[31] Prehn, R. T., J. M. Main. 1957. Immunity to methylcholanthrene-induced sarcomas. J. Natl. Cancer Inst, 18: 769C778.

[32] K. E. Johnson, G. Howard, W. Mo, et al., Cancer cell population growth kinetics at low densities deviate from the exponential growth model and suggest an allee effect, PLoS biology, 17 (2019), e3000399.

[33] K. S. Korolev, J. B. Xavier, J. Gore, Turning ecology and evolution against cancer, Nat. Rev. Cancer, 14 (2014), 371C380.

[34] K. Böttger, H. Hatzikirou, A. Voss-Böhme, et al., An emerging allee effect is critical for tumor initiation and persistence, PLoS Comput. Biol., 11 (2015), e1004366.

[35] D. S. Boukal, L. Berec, Single-species models and the Allee effect: extinction boundaries, sex ratios and mate encounters, Journal of Theoretical Biology, 218(2002) 375-394.

[36] C. W. Clark, Mathematical Bioeconomic. The Optimal Management of Renewable Resources, 2nd ed., John Wiley and Sons, New York, 1990.

[37] M. A. Wilson and L. M. Schuchter, Chemotherapy for melanoma, Cancer Treat. Res., 167(2016), pp. 209–229.

[38] McKay MD, Beckman RJ, Conover WJ (1979) Comparison of three methods for selecting values of input variables in the analysis of output from a computer code. Technometrics 21(2):239C245.

[39] Marino S, Hogue IB, Ray CJ, Kirschner DE (2008) A methodology for performing global uncertainty and sensitivity analysis in systems biology. Journal of theoretical biology 254(1):178C196.

[40] Liao, K. L., Bai, X. F., Friedman, A. (2014). Mathematical modeling of interleukin-35 promoting tumor growth and angiogenesis. PloS One, 9(10), e110126.

[41] Roesch, K., Hasenclever, D., Scholz, M. (2014). Modelling lymphoma therapy and outcome. Bulletin of Mathematical Biology, 76(2), 401C430.

[42] Kuznetsov, V. A., Makalkin, I. A., Taylor, M. A., Perelson, A. S. (1994). Nonlinear dynamics of immunogenic tumors: Parameter estimation and global bifurcation analysis. Bulletin of Mathematical Biology, 56(2), 295C321.

[43] Kronik, N., Kogan, Y., Elishmereni, M., Halevi-Tobias, K., Vuk-Pavlovic, S., Agur, Z. (2010). Predicting outcomes of prostate cancer immunotherapy by personalized mathematical models. PLoS One, 5(12), e15482.

[44] de Pillis, L. G., Radunskaya, A. E., Wiseman, C. L. (2005). A validated mathematical model of cell-mediated immune response to tumor growth. Cancer Research, 65(17), 7950C7958.

[45] Delitala M, Ferraro M. Is the Allee effect relevant in cancer evolution and therapy?. AIMS Mathematics. 2020;5(6):7649-60.

[46] López, á., Seoane, J., Sanjuán, M. (2014). A validated mathematical model of tumor growth including tumor-host interaction, cell-mediated immune response and chemotherapy. Bulletin of Mathematical Biology, 76(11), 2884C2906.

[47] Saltelli A, Sobol IM (1995) About the use of rank transformation in sensitivity analysis of model output. Reliability Engineering System Safety 50(3):225C239.

[48] Arciero, J. C., Jackson, T. L., Kirschner, D. E. (2004). A mathematical model of tumor-immune evasion and siRNA treatment. Discrete and Continuous Dynamical Systems Series B, 4(1), 39C58.

[49] Gonzlez-Olivares, E. D. U. A. R. D. O., et al. "Modelling the Allee effect: are the different mathematical forms proposed equivalents." Proceedings of the International Symposium on Mathematical and Computational Biology BIOMAT. Vol. 2007. 2006.